Author(s): Aalto, Sanni L.; Suurnäkki, Suvi; von Ahnen, Mathis; Siljanen, Henri M. P.; Pedersen, Per Bovbjerg; Tiirola, Marja

Title: Nitrate removal microbiology in woodchip bioreactors : a case-study with full-scale bioreactors treating aquaculture effluents

Year: 2020

Version: Accepted version (Final draft)

Please cite the original version:

Aalto, S. L., Suurnäkki, S., von Ahnen, M., Siljanen, H. M. P., Pedersen, P. B., & Tiirola, M. (2020). Nitrate removal microbiology in woodchip bioreactors : a case-study with full-scale bioreactors treating aquaculture effluents. Science of the Total Environment, 723, Article 138093. https://doi.org/10.1016/j.scitotenv.2020.138093

Journal Pre-proof

Nitrate removal microbiology in woodchip bioreactors: A case-study with full-scale bioreactors treating aquaculture effluents

Sanni L. Aalto, Suvi Suurnäkki, Mathis von Ahnen, Henri M.P. Siljanen, Per Bovbjerg Pedersen, Marja Tiirola

PII: S0048-9697(20)31606-5

DOI: https://doi.org/10.1016/j.scitotenv.2020.138093

Reference: STOTEN 138093

To appear in: *Science of the Total Environment*

Received date: 14 February 2020

Revised date: 19 March 2020

Accepted date: 19 March 2020

Please cite this article as: S.L. Aalto, S. Suurnäkki, M. von Ahnen, et al., Nitrate removal microbiology in woodchip bioreactors: A case-study with full-scale bioreactors treating aquaculture effluents, *Science of the Total Environment* (2018), https://doi.org/10.1016/j.scitotenv.2020.138093

Nitrate removal microbiology in woodchip bioreactors: a case-study with full-scale bioreactors treating aquaculture effluents

Sanni L. Aalto[1,2], Suvi Suurnäkki[2], Mathis von Ahnen[1], Henri M. P. Siljanen[3], Per Bovbjerg Pedersen[1], and Marja Tiirola[2]

[1]Technical University of Denmark, DTU Aqua, Section for Aquaculture, The North Sea Research Centre, P.O. Box 101, DK-9850 Hirtshals, Denmark

[2]Department of Biological and Environmental Science, Nanoscience Center, University of Jyväskylä, P.O. Box 35, 40014 Jyväskylä, Finland

[3]Department of Environmental and Biological Sciences, University of Eastern Finland, P.O. Box 1627, 70211 Kuopio, Finland

Corresponding author: Sanni L. Aalto, sheaa@aqua.dtu.dk

Running title: Microbial nitrate reduction in woodchip bioreactors

Keywords: denitrification, DNRA, nitrogen removal, nitrous oxide, recirculation aquaculture systems

Abstract

Woodchip bioreactors are viable low-cost nitrate (NO_3^-) removal applications for treating agricultural and aquaculture discharges. The active microbial biofilms growing on woodchips are conducting nitrogen (N) removal, reducing NO_3^- while oxidizing the carbon (C) from woodchips. However, bioreactor age, and changes in the operating conditions or in the microbial community might affect the NO_3^- removal as well as potentially promote nitrous oxide (N_2O) production through either incomplete denitrification or dissimilatory NO_3^- reduction to ammonium (DNRA). Here, we combined stable isotope approach, amplicon sequencing, and captured metagenomics for studying the potential NO_3^- removal rates, and the abundance and community composition of microbes involved in N transformation processes in the three different full-scale woodchip bioreactors treating

recirculating aquaculture system (RAS) effluents. We confirmed denitrification producing di-nitrogen gas (N_2) to be the primary NO_3^- removal pathway, but found that 6% of NO_3^- could be released as N_2O under high NO_3^- concentrations and low amounts of bioavailable C, whereas DNRA rates tend to increase with the C amount. The abundance of denitrifiers was equally high between the studied bioreactors, yet the potential NO_3^- removal rates were linked to the denitrifying community diversity. The same core proteobacterial groups were driving the denitrification, while Bacteroidetes dominated the DNRA carrying microbes in all the three bioreactors studied. Altogether, our results suggest that woodchip bioreactors have a high genetic potential for NO_3^- removal through a highly abundant and diverse denitrifying community, but that the rates and dynamics between the NO_3^- removal pathways depend on the other factors (e.g., bioreactor design, operating conditions, and the amount of bioavailable C in relation to the incoming NO_3^- concentrations).

1 Introduction

Food production is globally increasing to meet needs of the growing human population, requiring novel sustainable production methods to supplement the traditional agriculture. Aquaculture is the fastest growing food production sector (FAO 2017), but like other sectors, aquaculture needs to address environmental sustainability to sustain future growth and development. A modern production technology for commercial aquaculture is land-based recirculating aquaculture systems (RAS), which are based on efficient water recycling through microbial biofilter systems. Concomitantly, RAS discharges are typically of relatively low volume but with increased nutrient concentrations, especially nitrate (NO_3^-) that needs to be removed before discharging to the recipient ecosystems.

Woodchip bioreactors are passive NO_3^- removal systems used for removing NO_3^- in groundwaters, agricultural tile drainage waters, and human and animal wastewaters (see Addy et al, 2016; references therein), and more recently, in RAS discharges (Lepine et al. 2016; von Ahnen et al. 2018). In woodchip bioreactors, NO_3^- removal is driven by the active microbial biofilm, to which woodchips

offer both growth surface and carbon (C) source (Lopez-Ponnada et al. 2017). In general, the nitrate-nitrogen (NO_3-N) removal rates are rather low (2-22 g NO_3-N/m^3/d; Schipper et al. 2010), the maximum rates being 39 g NO_3-N/m^3/d (Lepine et al. 2016), in woodchip bioreactors treating nitrate-rich RAS effluents.

The primary NO_3^- removal process in woodchip bioreactors is considered to be denitrification, where NO_3^- is reduced into inert di-nitrogen gas (N_2), and thereby removed from the water. Denitrification is a sequential process with four enzymatic steps, and the genes coding for enzymes reducing nitrite (NO_2^-) to nitric oxide (NO), *nir*S and *nir*K, are the most widely used molecular markers to study denitrifier populations. Previously, *nir* gene abundance has been found to increase with NO_3-N removal rates in experimental denitrification beds including woodchips (Warneke et al. 2011) and in laboratory-scale woodchip bioreactors treating RAS effluents (von Ahnen et al. 2019), but knowledge on the abundance and communities of microbes carrying these genes under less-controlled full-scale woodchip bioreactors is currently missing. Denitrification can also be incomplete, producing nitrous oxide (N_2O) instead of N_2. The C availability is one of the key factors regulating N_2O yield (the proportion of incomplete denitrification of total denitrification), as high N_2O formation has been found under low C availability and high NO_3^- concentrations (low C: NO_3^-) in municipal wastewater systems (Spinelli et al. 2018). Although the measured bulk N_2O fluxes are usually low in woodchip bioreactors (Woli et al. 2010; Healy et al. 2012; Davis et al. 2019), the share of N_2O produced during denitrification is not known.

Woodchip bioreactors may also host microbes carrying out dissimilatory NO_3^- reduction to ammonium (DNRA), a process that retains nitrogen in the system as biologically reactive ammonium (NH_4^+). High C concentrations in relation to NO_3^- availability are considered to favour DNRA over denitrification (Kraft et al. 2014, Hardison et al. 2015), since DNRA bacteria generate more energy per mol of NO_3^- metabolized than denitrifiers. The role of DNRA is considered to be minor (4-9%) in woodchip bioreactors, based on earlier experiments with systems treating groundwater (Gibert et al.

2008), agricultural drainage water (Greenan et al. 2006), and household effluents (Warneke et al. 2011). However, recently, relatively high abundance of *nrf*A gene coding for DNRA process and increasing NH_4^+ concentrations were found in laboratory woodchip bioreactors (Grießmeier et al. 2017). Furthermore, DNRA microbes have been found in polymer denitrification systems treating RAS effluents under high residual C concentrations (Zhu et al. 2015). This suggests that DNRA could have a contribution to NO_3- removal also in the woodchip bioreactors treating RAS effluents, when most of the NO_3^- has been removed and the C:NO_3^- ratios increase.

Here, the nitrate reduction in three different full-scale woodchip bioreactors installed at commercial RAS farms (von Ahnen et al. 2018) was examined. It was hypothesized that the bioreactor nitrate reduction rates are related to the abundance and/or community composition of microbes and to the operation conditions. In order to get a comprehensive understanding on the interactions between the two competing NO_3^- reduction pathways, denitrification and DNRA, and controlling factors, a stable isotope approach for measuring potential process rates, and quantitative polymerase chain reaction (qPCR) for measuring the abundance of denitrification and DNRA genes were used. Since fungal denitrification can be a significant source for N_2O (Maeda et al. 2015), the abundance of fungal *nir*K gene was also measured. Furthermore, next generation sequencing targeted at *nir*S and *nir*K genes, and captured metagenomics for quantifying and characterizing the microbes involved in denitrification, as well as other nitrogen (N) transformation processes in woodchip bioreactors were performed.

2 Materials and methods

2.1 Full-scale bioreactors

The three woodchip bioreactors studied containing 250, 650, and 1250 m^3 of woodchips, respectively, treated the effluents from three commercial, Danish freshwater RAS rearing rainbow trout (*Oncorhynchus mykiss*) (Table 1; described in detail in von Ahnen et al. 2018). The woodchip bioreactors were filled with different blends of wood species containing amongst others spruce

(Picea sp.), poplar (Populus sp.), and beech (Fagus sp.) and were operated at hydraulic retention times ranging from 10 to 18 hours (Table 1).

2.2 Sampling and water chemistry analysis

Samples for water chemistry measurements were collected from inlet, outlet, and within the woodchip bioreactors in October 2017 and March 2018. Water for the microbiological analysis was collected using syringe filters (0.22 µm Millipore Express® PLUS PES membrane) from the same sampling points. In addition, woodchips were collected by hand from the subsurface layer of the bioreactor for stable isotope incubations and microbiological analysis of the woodchip biofilms (only in October 2017). In October 2017, the bioreactor water and woodchip samples were collected from one sampling point in the middle of the bioreactor. In March 2018, the bioreactor samples were collected from three different sampling points along the length of the bioreactor in order to capture the possible variation in the microbiology and processes within the bioreactor. All samples were kept on ice until the laboratory, and microbiological samples were frozen immediately after the sampling at -20°C.

Temperature, dissolved oxygen concentration, and pH were measured at the sampling points in March 2018 using a portable multimeter (Hach Lange HQ40 multimeters, Düsseldorf, Germany). For inorganic nutrient analysis, water samples were kept cold (+4°C) until further analysis. Samples were filtered through 0.2 µm syringe filters (Filtropur S 0.2 µm, Sarstedt, Germany) prior to analyses of total ammonia nitrogen (TAN; DS224, 1975; only in October 2017) and measurements of the ions nitrite-N (NO_2-N), and NO_3-N, using an ion chromatograph (Thermo Scientific™ Dionex™ Ion Chromatography, Mettler Toledo). The five-day biological oxygen demand from dissolved material (BOD_{5_diss}) was measured according to ISO 5815-2 (2003). For dissolved organic C (DOC; mg L^{-1}) and SUVA (specific ultraviolet absorbance, measured at 254 nm) measurements, samples were filtered after sampling with GF/F filters, and stored in brown precombusted glass bottles until analysis. Dissolved organic C was analyzed with Shimadzu TOC-LCPH total OC analyzer (Shimadzu, Japan). For

SUVA, spectrophotometric analyses of colored dissolved organic matter (CDOM) samples were performed using a UV-visible Cary 100 spectrophotometer (Agilent, Santa Clara, California) with 1 cm quartz cuvette over the spectral range from 250 to 800 nm with 1 nm intervals. After subtracting the blank spectrum, SUVA values were calculated by dividing the UV absorbance measured at 254 nm by the DOC concentration, and are reported in the units of square meters per gram C. Removal rates of NO_3-N, NO_2-N, TAN, BOD_{5_diss}, and DOC were calculated as in von Ahnen (2018).

2.3 Measurements of potential nitrate reduction rates

For measuring potential complete denitrification (N_2 production), incomplete denitrification (N_2O production), and DNRA rates, approximately 200 mL of woodchip were transferred into a 700-mL-volume incubation bottle), which was then filled with water collected from each woodchip bioreactor inlet. Incubation bottles were closed with septa caps and flushed with helium for 30 min to create anoxic conditions. After that, labelled NO_3^- (99% $^{15}NO_3^-$; Sigma Aldrich) was added to the final concentration of 5 mg/L in October 2017 and 10 mg/L in March 2018. In October 2017, three replicates and one unlabeled control incubation bottle were used, whereas in March 2018, one unlabeled control bottle and three incubation bottles representing the different sampling points in the woodchip bioreactor were used. Bottles were incubated in the dark for four hours at temperature of +18°C and under mixing of 50 rpm. After the incubation, bottles were shaken, and samples taken for stable isotope analysis. For the analysis of the isotopic composition of N_2 ($^{29}N_2$, $^{30}N_2$), three replicate water samples of 12 mL were collected to glass vials (Exetainer, Labco Scientific) filled with 0.5 mL $ZnCl_2$ (100% w/v, Merck), and analyzed with Isoprime IRMS connected to Tracegas preconcentrator unit as described in Aalto et al. (2018). For the isotopic analysis of N_2O ($^{45}N_2O$, $^{46}N_2O$), water sample of 30 mL was collected with a syringe and treated and analyzed as in Aalto et al. (2018). For DNRA measurement, 20 mL of water was filtered through cellulose acetate and glass fiber filters (CA-GF Filtropur S plus 0.2 µm, Sarstedt) and stored frozen (-20 °C) until $^{15}NH_4^+$ analysis. The NH_4^+ in the samples was converted to N_2 with alkaline hypobromite iodine solution

(Risgaard-Petersen et al. 1995), where 4 mL of sample was flushed with helium for 5 min, after which 100 µL alkaline hypobromite iodine solution was added. Vials were shaken overnight at room temperature, and subsequently N_2 was measured with an Isoprime IRMS. The potential production rates of N_2, N_2O, and DNRA, as well as relative N_2O ($\%N_2O$) and DNRA (%DNRA) rates, were calculated as in Aalto et al. (2018).

2.4 qPCR of denitrification and DNRA genes

DNA was extracted from water filters and biofilm samples with a PowerLyzer PowerSoil DNA extraction kit (MoBio Laboratories, Inc.). Before extraction, the microbial biofilm was detached from the surface of the woodchips by adding 20 ml of water to the sample tube, and sonicating in two periods of two minutes by an ultrasonic bath (Branson 1510). After that, woodchips were discarded, and biofilm samples were freeze-dried (Alpha 1-4 LD plus, Christ). The abundance of *nir*K (nirK876/1040; Henry et al. 2004), *nir*S (nirSC3aF/R3cd; Kandeler et al. 2006), fungal *nir*K (EunirKF1/R2; Maeda et al. 2015), *nosZ*$_{I}$ (nosZ2F/2R; Henry et al. 2006), *nosZ*$_{II}$ (nosZII;-F/R; Jones et al. 2013), and *nrf*A (NrfAFaw/R1; Mohan et al. 2004, Welsh et a al. 2014) genes in samples were quantified by qPCR amplification with Bio-Rad CFX96 Real-Time System (Bio-Rad Laboratories). The qPCR reactions of 25 µl consisted of Maxima SYBR Green/Fluorescein qPCR Master Mix (Thermo Fisher Scientific) and 5 ng of template DNA. Primer concentrations and detailed amplification protocols are listed in Table A.1. Amplification efficiencies were between 81-97% (fungal *nir*K 97%, *nir*K 96%, *nir*S 83%, *nrf*A 94%, *nos*Z$_{I}$ 90%, and *nos*Z$_{II}$ 81%). The standard curves were prepared from amplification products amplified with the corresponding primers. The amplification products were run on agarose gel, extracted using GenElute™ Agarose Spin Column (Sigma-Aldrich), and a minimum of five products were pooled together with equal volumes and purified with Agencourt AMPure XP purification system (Beckman Coulter Life Sciences, Indianapolis, IN, USA. Dilution series of 10^1-10^7 gene copies was prepared and used in the qPCR assays for each studied gene.

2.5 Denitrifier community composition

Changes in the community composition, richness, and diversity of organisms harbouring *nir*S or *nir*K gene were studied with next generation sequencing using samples collected in October 2017. To build the PCR amplicon libraries, two PCR reactions were performed. In the first PCR, primer pairs nirK876/1040 (Henry et al. 2004) and nirSC3aF/R3cd (Kandeler et al. 2006) were used with the M13 sequence (5'-TGTAAAACGACGGCCAGT-3') linker attached to the 5' end of each forward primer. The first reaction mixture of 25 µl contained 5 ng of DNA template, 0.4 µM *nir*S/0.5 µM *nir*K primers, and 1 x Maxima SYBR Green qPCR Master Mix. The PCR conditions were identical with qPCR quantifications above. In the second PCR, one µl of the PCR I product was used as a template, and Ion Torrent PGM sequencing adapters and barcodes were added to the ends of PCR product using linker and fusion primers (0.04 µM of M13_515F-Y, 0.4 µM of IonA_IonXpressBarcode_M13 and P1_806R) in ten additional cycles with conditions otherwise identical to the first amplification. Products were purified with Agencourt AMPure XP purification system, quantified, and pooled in equimolar quantities for sequencing on Ion Torrent PGM using Ion PGM Hi-Q View OT2 Kit for emulsion PCR, PGM Hi-Q View Sequencing Kit for the sequencing reaction and Ion 316 Chip v2 (all Life Sciences, Thermo Fisher Scientific).

Analysis of gene sequences was done using mothur (version 1.39.5; Schloss et al. 2009). Sequences shorter than 150 bp, low-quality sequences with more than one mismatch in barcode/primer sequences, or with homopolymers longer than eight nucleotides, as well as barcodes, and primers were removed. Framebot (Wang et al. 2013) was used to correct frameshift errors, and sequences were aligned with sets of aligned *nir*S and *nir*K sequences retrieved from the FunGene (Fish et al. 2013). Chimeric sequences, denoted using mothur's implementation of Uchime (Edgar et al. 2011), were removed from each library. Sequences were divided into operational taxonomic units (OTUs) at 95% similarity levels, and singleton OTUs (OTUs with only one sequence in the entire dataset) were removed. Finally, the data was normalized by subsampling to 2383 for *nir*S and 7672 for *nir*K for

calculating Shannon diversity index and chao OTU richness estimate. Sequence variation was adequately covered in these libraries as shown by Good's coverage, an estimate of the proportion of amplified gene amplicons represented by sequence libraries for each sample, that varied 0.93-0.98 for *nir*S, and 0.98-1.00 for *nir*K. Sequences have been submitted to NCBI Sequence Read Archive under BioProject PRJNA553058.

2.6 Captured metagenomics of nitrogen cycling microbes

In captured metagenomics done for biofilm samples collected in October 2017, the organisms carrying nitrogen cycling genes involved in N_2 fixation, nitrification, NO_3^- reduction, denitrification, and DNRA were targeted and sequenced using gene specific probes following the NimbleGen SeqCap EZ protocol by Roche NimbleGen, Inc.. The method is described in detailed in the Appendix A.

2.7 Statistical analysis

All statistical analyses were conducted using R version 3.5.1 (R Core Team, 2018). Non-metric multidimensional scaling (NMDS, conducted with metaMDS function in vegan package; Oksanen et al. 2015) plots calculated based on Bray–Curtis distance matrix were used to visualize dynamics in the *nir*S and *nir*K community structures. Before NMDS, Wisconsin and square- root-transformations were applied to OTU abundance data. The differences in the *nir*S and *nir*K community compositions between the bioreactors and the sampling points were examined with the permutational analysis of variance (PERMANOVA). The correlations between potential NO_3^- reduction rates, inorganic N concentrations, and C variables, and/or abundance of denitrification and DNRA genes, and *nir*S and *nir*K diversity (Shannon) and OTU richness (chao) were examined with Spearman correlation analysis.

3 Results

All three bioreactors removed NO_3-N, the rates varying between 2.34 and 8.20 g NO_3-N/m^3/d (Table 2). Nitrite was either produced or removed in low rates, while low TAN removal rates (0.50-1 g

TAN/m^3/d) were found in all bioreactors (Table 2). Organic matter (described as BOD_{5_diss} or DOC) was produced in bioreactor 1 on both sampling dates, and in bioreactor 2 in October 2017, but was removed in bioreactor 2 in March 2018 and in bioreactor 3 on both sampling dates. The specific ultraviolet absorbance (SUVA) index was measured only in March 2018, being higher in bioreactor 2 than in other two bioreactors. Oxygen was quickly consumed, and pH declined from inlet to outlet in all three bioreactors (Table A.2). The water temperature was between 10-13°C in October 2017 and 6-9°C in March 2018.

3.1 NO_3-N removal pathways

The potential NO_3^- reduction rates (g N/m^3 woodchip/d) measured with stable isotope incubations were lowest in bioreactor 1, which had the lowest incoming NO_3-N concentration (Figure 1), corresponding approximately to the calculated average volumetric NO_3-N removal rates. There was a substantial variation in the relative proportions of three NO_3^- reduction pathways between the bioreactors and sampling dates, but complete denitrification producing N_2 was still the primary NO_3^- reduction process (89-93% in October 2017, 76-85% in March 2018). The potential incomplete denitrification rates (N_2O production) varied between 1-6% of total NO_3^- reduction in October 2017, and were <1% in March 2018. The potential rates of DNRA comprised 5- 9% of total NO_3^- reduction in October 2017 and 14-23 % in March 2018.

In October 2017, the potential N_2 production was not related to the incoming NO_3-N concentrations and was negatively correlated with BOD_5, but in March 2018, the potential N_2 production increased with increasing NO_3-N and DOC concentrations (Spearman correlation, NO_3^-: $\rho = 0.84$, $p < 0.001$, DOC: $\rho = 0.62$, $P = 0.002$; Table A.3). On both sampling dates, the potential N_2O production rate and the relative N_2O production increased with increasing NO_3-N ($\rho = 0.45$-0-79, $p < 0.05$), and in March 2018, decreased when DOC was higher ($\rho = -0.83$, $P < 0.001$), leading to highest N_2O production at low DOC:NO_3^- ratio. Furthermore, the potential N_2O production was higher when the organic matter was less bioavailable (high SUVA index values; $\rho = 0.60$-0.65, $P < 0.05$). The potential DNRA rate

increased with DOC concentration (ρ = 0.73, P < 0.001), and under high DOC:NO_3^-, both actual and relative potential DNRA rates were high.

3.2 Genetic potential for denitrification and DNRA

The abundance of the denitrification genes (*nir*S, *nir*K, *nos*Z_I, *nos*Z_{II}) and DNRA gene (*nrf*A) was higher in the samples taken from within the woodchip bioreactor than in the inlet or the outlet (Table 3). In addition, the abundance of *nir* and *nos* was higher in the woodchip biofilm samples than in the water samples in October 2017. The abundance of *nir* genes was higher than that of the other genes on both sampling dates. The abundance of *nos*Z_I was higher in March 2018 than in October 2017, whereas *nos*Z_{II} abundance exhibited an opposite pattern. The abundance of *nrf*A remained rather similar between the two sampling dates (Table 3). No copies of fungal *nir*K were found in any of the bioreactors.

Since there was some variation in the gene abundances between the sampling dates, their interactions with NO_3^- reduction rates were examined separately. We focused on the genetic potential for N_2O production (*nir/nos*) and the relationships between genetic potential of DNRA and denitrification (*nrf*A/*nir*), instead of the absolute gene copy numbers. The genetic potential for N_2O production (*nir/nos*) was positively related to the actual and relative potential N_2O production in March 2018 (Spearman correlation, N_2O: ρ = 0.76, P < 0.001; %N_2O: ρ = 0.49, P = 0.021; Table A.3). In both water and biofilm samples, a positive relationship between *nrf*A/*nir* and DNRA or %DNRA was found, indicating that when the *nrf*A/*nir* was higher, DNRA rates increased (ρ = 0.57-0.92, P < 0.05; Table A.3).

3.3 Nitrogen transforming microbial communities

The compositions of the *nir*S and *nir*K communities were significantly different between the three bioreactors studied (PERMANOVA, nirS: F = 2.4, p = 0.002; nirK: F = 2.8, P = 0.003; Figure 2). For *nir*S, water and woodchip biofilm communities were different from the inlet and outlet communities (F = 1.7, P = 0.018). In bioreactors 1 and 2, the diversity and species richness of *nir*S decreased from inlet

to woodchip bioreactor samples, whereas *nir*K diversity and richness increased from inlet to bioreactor water and biofilm samples. In bioreactor 3, the diversity and richness of both communities increased from inlet to bioreactor biofilm samples (Table 3). In water and biofilm samples, *nir*S diversity and species richness were high when potential DNRA and N_2 production rates were high (ρ = 0.65-0.98, $P < 0.05$), and the high *nir*K diversity and/or species richness coincided with high actual and relative potential N_2O production rates (ρ = 0.68-0.76, $P < 0.05$; Table A.3).

Using the novel captured metagenomics tool, the microbes carrying genes involved in nitrification (archaeal *amo*A, bacterial *amo*A, *nxr*B), anammox (*hzo*A), nitrogen fixation (*nif*H), denitrification (NO_3^- reductases: *nap*A*, nar*G; NO_2^- reductases: *nir*K*, nir*S; nitric oxide reductase: *nor*B; N_2O reductase: *nos*Z), and DNRA (*nrf*A) could be quantified and identified in woodchip biofilm samples in October 2017. The abundance of sequences related to NH_4^+ oxidation and anammox was very low (*amo*A*:* <200 seqs: *hzo*A: <5 seqs), and the abundance of *nxr*B carrying microbes varied between 15,000 and 20,000 seqs (data not shown). The quantity of sequences related to N_2 fixation was very high (141,729-255,033 seqs; Figure A.1a), and the communities were diverse, the most abundant bacterial orders being proteobacterial Acidithiobacillales, Desulfovibrionales, and Rhodocyclales, and photoautotrophic Chlorobiales from Phylum Chlorobi in all bioreactors. The abundance of DNRA-carrying microbes was low as compared to denitrifiers (0.6-0.9% of sequences related to denitrification and DNRA; Figure 3a), but the communities were diverse, including members from classes Bacteroidia, Campylobacteria, and Delta-and Gammaproteobacteria. The most abundant *nrf*A order was Bacteroidales at all sites (Figure 3b). The relative abundances of NO_3^- (sum of *nap*A and *nar*G; 34-39% of sequences related to denitrification and DNRA) and NO_2^--reducing microbes (sum of *nir*K and *nir*S; 38-40%) were similar between the bioreactors, while the relative abundance of the microbes carrying the other two denitrification genes varied between the bioreactors, the abundance of *nor*B-carrying (N_2O-producing) microbes being higher (14% vs. 8-10%) and the abundance of *nos*Z-carrying (N_2O-consuming) microbes being lower (9% vs. 16%) in bioreactor 2 than in other bioreactors (Figure 3a). The *nar*G community was dominated by

gammaproteobacterial Enterobacteriales and *nor*B community by betaproteobacterial Pseudomonadales in all bioreactors (Figure A.1). The *nap*A communities were more diverse, the dominant orders were betaproteobacterial Burkholderiales and Rhodocyclales, and alphaproteobacterial Rhodospirillales in all bioreactors (Figure A.1). In the *nir*K, *nir*S and *nos*Z communities, the key orders were betaproteobacterial Burkholderiales and Pseudomonadales, and alphaproteobacterial Rhizobiales and Rhodobacterales (Figure 3b). The estimated *nir*K and *nir*S communities diversities were similar between the bioreactors, while bioreactor 1 had lower *nos*Z and higher *nrf*A diversity than other bioreactors (Figure A.2).

4 Discussion

In this study, the denitrification producing N_2 was confirmed to be the primary NO_3^- reduction pathway in the woodchip bioreactors treating RAS effluents (Figure 1). However, the potential for N_2O production and DNRA was also found in all three woodchip bioreactors. The N_2O production rates were generally low (max. 1% of total NO_3^- reduction), but in bioreactor 2 in October 2017, 6% of NO_3^- reduced was removed as N_2O (249±28 mg $N/m^3/d$). The potential DNRA rates varied between 5-23% of total NO_3^- reduction, the highest potentials found in bioreactor 3 in March 2018.

In woodchip bioreactors, NO_3-N removal rates are generally dependent on hydraulic retention time as well as inlet NO_3-N concentrations (Addy et al. 2016; Lepine et al. 2016; Martin et al. 2019). Here, neither denitrification producing N_2 nor DNRA were found to be related to NO_3-N concentration in October 2017, suggesting that other factors, such as C availability (Maxwell et al. 2019) or temperature (Lepine et al. 2016), limited these processes. However, in March 2018, the rates of both denitrification and DNRA were found to increase with the increasing incoming NO_3-N concentration. In addition, the process rates were related to DOC, highlighting the importance of C availability for these heterotrophic processes. The rate of denitrification producing N_2O increased with the incoming NO_3-N concentrations on both sampling dates. Furthermore, both actual and relative N_2O production increased with the decreasing amount of bioavailable C (increasing SUVA index), and the

relative N_2O production also increased when bulk C availability (DOC concentration) was low (Table A.3). These results suggest that N_2O production was related to the amount of bioavailable C in relation to NO_3-N in these bioreactors. Indeed, the accumulation of N_2O is observed under high NO_3^- concentration and low C availability, the electron consumption rate of *nos* being the lowest of all the denitrifying enzymes (Zhao et al. 2019). Since N_2O production was highest and the amount of bioavailable C lowest in the bioreactor with the shortest operational age (bioreactor 2; Figure 1, Table 2), it is possible that C bioavailability changes with bioreactor operational age (Abusallout & Hua 2017), but more comprehensive studies are needed to verify this, as well as the role of C quantity and quality in controlling N_2O production in general.

In addition to denitrification, the relationship between bioavailable C and NO_3^- could explain why a higher share of DNRA was found in bioreactor 1, which is known to be NO_3^- limited and produced excess amount of C (von Ahnen et al. 2018), conditions potentially favouring DNRA bacteria (Kraft et al. 2014, Hardison et al. 2015). It seems that NO_3^- limitation in these woodchip bioreactors can be problematic not only due to the risk of increased hydrogen sulphide production through sulphate reduction, and increased dissolved organic matter release (Schipper et al. 2010; Christianson et al. 2017; von Ahnen et al. 2018), but also due to the higher proportions of N being retained and discharged as TAN. Therefore, the hydraulic retention times of the woodchip bioreactors should correspond to the incoming NO_3^- loading, temperatures and expected NO_3- removal rates, not aiming for concentrations below 3 mg NO_3-N/l in the outlet.

Recently, the NO_3- removal rates were found to increase with the increasing abundance of NO_3^--reducing microbes in vegetated woodchip bioreactors (Fatehi-Pouladi et al. 2019). Here, the NO_3-N removal rates were not directly related to the abundance of microbes carrying denitrification/DNRA genes, which was similar among the three bioreactors (Table 3). This is explained with the denitrifying microbes being a functionally diverse group, which includes microbes carrying only the first part of denitrification pathway or DNRA (Graf et al. 2014; Decleyre et al. 2016). In order to

examine the dynamics between different NO_3^- reduction pathways, the genetic potential of DNRA and denitrification was assessed with the ratio between the abundance of *nrf*A and *nir* (Putz et al. 2018), and the genetic N_2O production potential with the ratio between *nir* and *nos* abundance (Saarenheimo et al. 2015). Although both ratios were much lower in March 2018 than in October 2017, presumably because not all of the highly abundant *nir* carrying microbes were true denitrifiers, *nrf*A/*nir* was found to correlate positively with DNRA rates and *nir/nos* with N_2O production rates, suggesting that the NO_3^- reduction pathway was at least partially related to the relative abundances of the microbes carrying these key genes.

In addition to microbial abundances, community composition of nitrate removing microbes can be reflected to NO_3^- removal rates, as has been shown in salt marsh sediments (Angell et al. 2018) or recently, in laboratory-scale woodchip bioreactors (von Ahnen et al. 2019). Based on *nir*S sequencing, the denitrifying communities within the bioreactors were found to be different from the ones found in the inlet and outlets (Figure 2), suggesting that the bioreactor communities develop in the same direction under the prevailing conditions and are less dependent on the operating conditions. This is corroborated by the captured metagenomics results, where the relative abundances of microbial orders carrying genes involved in denitrification and DNRA were similar between the bioreactors (Figure 3a). The small differences found in the abundance of the key denitrifying groups (betaproteobacterial Burkholderiales and Pseudomonadales, and alphaproteobacterial Rhizobiales and Rhodobacterales; Figure 3) are presumably explained by differences in the NO_3^- concentrations between the bioreactors (Grießmeier et al. 2017), or by woodchip species. However, both N_2 production and DNRA rates increased when the diversity and richness of the abundant *nir*S-carrying denitrifiers increased. Furthermore, the *nos*Z diversity was higher and *nrf*A diversity lower in bioreactors 2 and 3 with high nitrate concentrations than in N-limited bioreactor 1. These findings suggest that high incoming NO_3^- concentrations do not directly promote abundance, but the denitrifying community diversity and richness, which is then reflected to the overall rates as well as the dynamics between the NO_3^- reduction processes.

5 Conclusions

In conclusion, our results show that the NO_3-N removal in the woodchip bioreactors is carried by the complete denitrification producing N_2, the measured potential rates reflecting the incoming NO_3-N loading as well as the microbial community. However, changes in the quantity of biodegradable C, not bulk C as expected, may promote N_2O production as well as the share of NO_3^- converted into NH_4^+ through DNRA, but more field data and laboratory experiments are needed to verify this. Based on the microbial analysis, all three woodchip bioreactors studied hosted active and abundant communities of core microbial taxa, although the operating conditions varied. However, the NO_3-N removal dynamics and rates were related to the diversity of denitrifying microbes and relative abundances of carrying the key denitrification and DNRA genes. There is a need to increase the volumetric N removal rate in woodchip bioreactors, to avoid excessive bioreactor volumes under larger effluent volumes (e.g. when RAS production units are getting larger). Higher N removal rates might be achieved by using vegetated woodchip bioreactors, where bioavailable C is leaching from woodchips and plants growing on woodchips (Fatehi-Pouladi et al. 2019), promoting the activity of denitrification microbes. Increased volumetric N removal would allow high RAS production in the spatially limited areas, and provide opportunities to couple blue and green bioeconomy, improving the sustainability of aquaculture, and food production sector in general.

Acknowledgements

The work was supported by the funding of BONUS CLEANAQ project for PBP, European Research Council (ERC) CoG project 615146 for MT, Academy of Finland project 310302 for SLA and 290315 for HS. We thank the laboratory technicians Ulla Sproegel, Brian Møller, Melissa Lyng, and Dorthe Frandsen (DTU Aqua), and Mervi Koistinen and Emma Pajunen (University of Jyväskylä) for the invaluable technical assistance in the laboratories and Elina Virtanen (University of Jyväskylä) for assisting in the high-throughput sequencing. We thank Maxime Waulthy and Milla Rautio (Université

du Québec à Chicoutimi) for offering assistance and facility for SUVA measurements. We thank the fish farmers for allowing us access to their facilities.

References

Aalto, S. L., Saarenheimo, J., Ropponen, J., Juntunen, J., Rissanen, A. J., & Tiirola, M. (2018). Sediment diffusion method improves wastewater nitrogen removal in the receiving lake sediments. Water Research, 138, 312-322.

Abusallout, I., & Hua. G. (2017). Characterization of dissolved organic carbon leached from a woodchip bioreactor. Chemosphere, 183, 36-43.

Addy, K., Gold, A. J., Christianson, L. E., David, M. B., Schipper, L. A., & Ratigan, N. A. (2016). Denitrifying bioreactors for nitrate removal: A meta-analysis. Journal of Environmental Quality, 45(3), 873-881.

Angell, J. H., Peng, X., Ji, Q., Craick, I., Jayakumar, A., Kearns, P. J., Ward, B. B, & Bowen, J. L. (2018). Community composition of nitrous oxide-related genes in salt marsh sediments exposed to nitrogen enrichment. Frontiers in Microbiology, 9, 170.

Christianson, L. E., Lepine, C., Sibrell, P. L., Penn, C., & Summerfelt, S. T. (2017). Denitrifying woodchip bioreactor and phosphorus filter pairing to minimize pollution swapping. Water Research, 121, 129-139.

Davis, M. P., Martin, E. A., Moorman, T. B., Isenhart, T. M., & Soupir, M. L. (2019). Nitrous oxide and methane production from denitrifying woodchip bioreactors at three hydraulic residence times. Journal of Environmental Management, 242, 290-297.

Decleyre, H., Heylen, K., Tytgat, B., & Willems, A. (2016). Highly diverse nirK genes comprise two major clades that harbour ammonium-producing denitrifiers. BMC Genomics, 17, 1-13.

Edgar, R. C., Haas, B. J., Clemente, J. C., Quince, C., & Knight, R. (2011). UCHIME improves sensitivity and speed of chimera detection. Bioinformatics, 27(16), 2194–2200.

FAO, 2017. Food and Agriculture Organization (FAO). Fisheries and Aquaculture Statistics. FAO Year Book. FAO, Rome, Italy.

Fatehi-Pouladi, S., Anderson, B. C., Wootton, B., Button, M., Bissegger, S., Rozema, L., & Weber, K. P. (2019). Interstitial water microbial communities as an indicator of microbial denitrifying capacity in wood-chip bioreactors. Science of The Total Environment, 655, 720-729.

Fish, J. A., Chai, B., Wang, Q., Sun, Y., Brown, C. T., Tiedje, J. M., & Cole R .J. (2013). FunGene: the functional gene pipeline and repository. Frontiers in Microbiology, 4(291), 1-14.

Gibert, O., Pomierny, S., Rowe, I., & Kalin, R. M. (2008). Selection of organic substrates as potential reactive materials for use in a denitrification permeable reactive barrier (PRB). Bioresource Technology, 99(16), 7587-7596.

Graf, D. R., Jones, C. M., & Hallin, S. (2014). Intergenomic comparisons highlight modularity of the denitrification pathway and underpin the importance of community structure for N_2O emissions. PloS One, 9(12), e114118.

Greenan, C. M., Moorman, T. B., Kaspar, T. C., Parkin, T. B., & Jaynes, D. B. (2006). Comparing carbon substrates for denitrification of subsurface drainage water. Journal of Environmental Quality, 35(3), 824-829.

Grießmeier, V., Bremges, A., McHardy, A. C., & Gescher, J. (2017). Investigation of different nitrogen reduction routes and their key microbial players in wood chip-driven denitrification beds. Scientific Reports, 7(1), 17028.

Hardison, A. K., Algar, C. K., Giblin, A. E., & Rich, J. J. (2015). Influence of organic carbon and nitrate loading on partitioning between dissimilatory nitrate reduction to ammonium (DNRA) and N_2 production. Geochimica et Cosmochimica Acta, 164, 146-160.

Healy, M. G., Ibrahim, T. G., Lanigan, G. J., Serrenho, A. J., & Fenton, O. (2012). Nitrate removal rate, efficiency and pollution swapping potential of different organic carbon media in laboratory denitrification bioreactors. Ecological Engineering, 40, 198-209.

Henry, S., Baudoin, E., López-Gutiérrez, J. C., Martin-Laurent, F., Brauman, A., & Philippot, L. (2004). Quantification of denitrifying bacteria in soils by nirK gene targeted real- time PCR. Journal of Microbiological Methods, 59(3), 327–335.

Henry, S., Bru, D., Stres, B., Hallet, S., & Philippot, L. (2006). Quantitave detection of *nos*Z gene, encoding nitrous oxide reductase, and comparison of the abundances of 16S rRNA, *nar*G, *nir*K, and *nos*Z genes in soils. Applied and Environmental Microbiology, 72, 5181-5189.

ISO 5815-2, 2003. Water Quality—Determination of Biochemical Oxygen Demand After N Days (BODn)—Part 2: Method for Undiluted Samples, ISO 5815-2:2003, Modified. International Organization for Standardization, Geneva, Switzerland.

Jones, C. M., Graft, D. R. H., Bru, D., Philippot, L., & Hallin, S. (2013). The unaccounted yet abundant nitrous oxide-reducing microbial community: a potential nitrous oxide sink. ISME Journal, 7, 417-426.

Kandeler, E., Deiglmayr, K., Tscherko, D., Bru, D., & Philippot, L. (2006). Abundance of narG, nirS, nirK, and nosZ genes of denitrifying bacteria during primary successions of a glacier foreland. Applied and Environmental Microbiology, 72(9), 5957-5962.

Kraft, B., Tegetmeyer, H. E., Sharma, R., Klotz, M. G., Ferdelman, T. G., Hettich, R. L., Geelhoed, J.S., & Strous, M. (2014). The environmental controls that govern the end product of bacterial nitrate respiration. Science, 345(6197), 676-679.

Lepine, C., Christianson, L., Sharrer, K., & Summerfelt, S. (2016). Optimizing hydraulic retention times in denitrifying woodchip bioreactors treating recirculating aquaculture system wastewater. Journal of Environmental Quality, 45(3), 813-821.

Lopez-Ponnada, E. V., Lynn, T. J., Peterson, M., Ergas, S. J., & Mihelcic, J. R. (2017). Application of denitrifying wood chip bioreactors for management of residential non-point sources of nitrogen. Journal of Biological Engineering, 11(1), 16.

Maeda, K., Spor, A., Edel-Hermann, V., Heraud. C., Breuil. M. C., Bizouard. F., Toyoda, S., Yoshida, N., Steinberg, C., & Philippot, L. (2015). N2O production. A widespread trait in fungi. Scientific Reports, 5, 9697.

Martin, E. A., Davis, M. P., Moorman, T. B., Isenhart, T. M., & Soupir, M. L. (2019). Impact of hydraulic residence time on nitrate removal in pilot-scale woodchip bioreactors. Journal of Environmental Management, 237, 424-432.

Maxwell, B. M., Birgand, F., Schipper, L. A., Christianson, L. E., Tian, S., Helmers, M. J., Williams, D. J., Chescheir, G. M., & Youssef, M. A. (2019). Drying–rewetting cycles affect nitrate removal rates in woodchip bioreactors. Journal of Environmental Quality, 48(1), 93-101.

Mohan, S. B., Schmid, M., Jetten, M. S. M. (2004). Detection and widespread distribution of *nrf*A gene encoding nitrite reduction to ammonia, a short circuit in the biological nitrogen cycle that competes with denitrification. FEMS Microbiology Ecology, 49, 433-443.

Oksanen, J., Blanchet, F. G., Kindt, R., Legendre, P., Minchin, P. R., O'Hara, R. B., Simpson, G. L., Solymos, P., Stevens, M. H. H., & Wagner, H. (2017). vegan: Community Ecology Package. R package version 2.3–0. 2015.

Putz, M., Schleusner, P., Rütting, T., & Hallin, S. (2018). Relative abundance of denitrifying and DNRA bacteria and their activity determine nitrogen retention or loss in agricultural soil. Soil Biology and Biochemistry, 123, 97-104.

R Core Team (2018). R: A language and environment for statistical computing. R Foundation for Statistical Computing, Vienna, Austria. URL https://www.R-project.org/.

Risgaard-Petersen, N., Revsbech, N. P., & Rysgaard, S. (1995). Combined microdiffusion-hypobromite oxidation method for determining nitrogen-15 isotope in ammonium. Soil Science Society of America Journal, 59(4), 1077-1080.

Saarenheimo, J., Rissanen, A. J., Arvola, L., Nykänen, H., Lehmann, M. F., & Tiirola, M. (2015). Genetic and environmental controls on nitrous oxide accumulation in lakes. PLoS One, 10(3), e0121201.

Schipper, L. A., Robertson, W. D., Gold, A. J., Jaynes, D. B., & Cameron, S. C. (2010). Denitrifying bioreactors—an approach for reducing nitrate loads to receiving waters. Ecological Engineering, 36(11), 1532-1543.

Schloss, P. D., Westcott, S. L., Ryabin, T., Hall, J. R., Hartmann, M., Hollister, E. B., Lesniewski, R. A., Oakley, B. B., Parks, D. H., Robinson, C. J., Sahl, J. W., Stres, B., Thallinger, G. G., van Horn, D J. & Weber, C. F. (2009). Introducing mothur: open- source, platform-independent, community-supported software for describing and comparing microbial communities. Applied and Environmental Microbiology, 75, 7537–7541.

Spinelli, M., Eusebi, A. L., Vasilaki, V., Katsou, E., Frison, N., Cingolani, D., & Fatone, F. (2018). Critical analyses of nitrous oxide emissions in a full scale activated sludge system treating low carbon-to-nitrogen ratio wastewater. Journal of Cleaner Production, 190, 517-524.

von Ahnen, M., Pedersen, P. B., & Dalsgaard, J. (2018). Performance of full-scale woodchip bioreactors treating effluents from commercial RAS. Aquacultural Engineering, 83, 130-137.

von Ahnen, M., Aalto, S. L., Suurnäkki, S., Tiirola, M., & Pedersen, P. B. (2019). Salinity affects nitrate removal and microbial composition of denitrifying woodchip bioreactors treating recirculating aquaculture system effluents. Aquaculture, 504, 182-189.

Warneke, S., Schipper, L. A., Matiasek, M. G., Scow, K. M., Cameron, S., Bruesewitz, D. A., & McDonald, I. R. (2011). Nitrate removal, communities of denitrifiers and adverse effects in different carbon substrates for use in denitrification beds. Water Research, 45(17), 5463-5475.

Wang, Q., Quensen, J. F. 3rd, Fish, J. A, Lee, T. K., Tiedje, J. M., & Cole, J. R. (2013). Ecological patterns of nifH genes in four terrestrial climatic zones explored with targeted metagenomics using FrameBot, a new informatics tool. Mbio, 4(5), e00592-13.

Welsh, A., Chee-Sanford, J. C., Connor, L. M., Löffler, F. E., Sanford, R. A. (2014). Refined NrfA phylogeny improves PCR-based *nrf*A detection. Applied and Environmental Microbiology, 80(7), 2110-2119.

Woli, K. P., David, M. B., Cooke, R. A., McIsaac, G. F., & Mitchell, C. A. (2010). Nitrogen balance in and export from agricultural fields associated with controlled drainage systems and denitrifying bioreactors. Ecological Engineering, 36(11), 1558-1566.

Zhao, Y., Zeng, D., & Wu, G. (2019). Efficient nitrous oxide production and metagenomics-based analysis of microbial communities in denitrifying systems acclimated with different electron acceptors. International Biodeterioration & Biodegradation, 138, 92-98.

Zhu, S. M., Deng, Y. L., Ruan, Y. J., Guo, X. S., Shi, M. M., & Shen, J. Z. (2015). Biological denitrification using poly (butylene succinate) as carbon source and biofilm carrier for recirculating aquaculture system effluent treatment. Bioresource technology, 192, 603-610.

Table legends

Table 1. The characteristics (mean ± SD) of the three woodchip bioreactors studied. EBCT = empty bed contact time, HRT = Hydraulic retention time. Modified from von Ahnen et al. (2018).

Table 2. Nitrate-nitrogen (NO_3-N), nitrite-nitrogen (NO_2-N), and total ammonia nitrogen (TAN) concentrations, five day biochemical oxygen demand (BOD_{5_diss}), dissolved organic carbon (DOC) concentrations and specific ultraviolet absorbance at 254 nm (SUVA) in inlet, outlet and within bioreactors (sampling points 1-3; SP1-3), and the average volumetric removal rates (RR) in the three bioreactors over the two sampling dates.

Table 3. Gene copy numbers (copies/mL water for water samples, copies/g of dw for biofilm samples), the relationship between DNRA and denitrification potential (*nrfA/nir*), the genetic potential for N_2O production (*nir/nos*), and the diversity and species richness of *nir*S and *nir*K communities in inlet and outlet water, and in water and biofilm within the bioreactors (sampling points 1-3; SP1-3) in the three bioreactors over the two sampling dates.

Figure legends

Figure 1. The potential rates of nitrate reduction processes (N_2: denitrification producing N_2, N_2O: denitrification producing N_2O, and DNRA) at three sampling points (SP1-3) in the three bioreactors (Bioreactor1-3) over the two sampling dates (October 17 and March 18).

Figure 2. Non-metric multidimensional scaling (NMDS) of a) *nir*K and b) *nir*S community compositions based on Bray–Curtis dissimilarities in water and biofilm samples in the three bioreactors.

Figure 3. The amount of reads assigned to genes involved in a) denitrification (*nap*A, *nar*G, *nir*K, *nir*S, *nor*B, *nos*Z) and DNRA (*nrf*A), and b) in nitrite reduction (*nir*K, *nir*S), N_2O reduction (*nos*Z), and DNRA

(*nrf*A), and their taxonomic assignment obtained with the captured metagenomics tool in woodchip biofilms in the three bioreactors in October 2017. Percentages denote for the relative abundance of the key orders (≥10% of reads per sample).

Credit author statement

Sanni L. Aalto: Conceptualization, Formal analysis, Investigation, Writing - Original Draft, Writing - Review & Editing, Visualization, Suvi Suurnäkki: Formal analysis, Investigation, Writing - Original Draft, Mathis von Ahnen: Investigation, Writing - Original Draft, Writing - Review & Editing, Henri M. P. Siljanen: Methodology, Formal analysis, Per Bovbjerg Pedersen: Conceptualization, Resources, Funding acquisition, Marja Tiirola: Conceptualization, Resources, Supervision, Funding acquisition

Declaration of interests

☒ The authors declare that they have no known competing financial interests or personal relationships that could have appeared to influence the work reported in this paper.

☐The authors declare the following financial interests/personal relationships which may be considered as potential competing interests:

Table 1. The characteristics (mean ± SD) of the three woodchip bioreactors studied. EBCT = empty bed contact time, HRT = Hydraulic retention time. Modified from von Ahnen et al. (2018).

	Bioreactor 1	Bioreactor 2	Bioreactor 3
Start of operation	March 2017	July 2017	January 2017
Length x width x depth (m)	30 × 10 × 1	30 × 20 × 1.1	60 × 20 × 1.2
Submerged woodchip volume (m^3)	250	650	1250
Inflow rate (L/s)	3 ± 2	12 ± 4	25 ± 4
Average EBCT (h)	26 ± 13	16 ± 4	15 ± 9
Average HRT (h)	18 ± 9	11 ± 3	10 ± 6
Direction of water flow	Horizontal	Vertical, down flow	Vertical, down flow

Table 2. Nitrate-nitrogen (NO_3-N), nitrite-nitrogen (NO_2-N), and total ammonia nitrogen (TAN) concentrations, five day biochemical oxygen demand (BOD_{5_diss}), dissolved organic carbon (DOC) concentrations and specific ultraviolet absorbance at 254 nm (SUVA) in inlet, outlet and within bioreactors (sampling points 1-3; SP1-3), and the average volumetric removal rates (RR) in the three bioreactors over the two sampling dates.

Bioreactor	Sampling date and bioreactor age (mo)	Sampling point	NO_3-N mg/L	NO_2-N mg/L	TAN mg/L	BOD_{5_diss} mg/L	DOC mg/L	SUVA m^2/g C
Bioreactor 1	October 2017 (7 mo)	inlet	5.02	0.11	1.10	2.40	na	
		outlet	1.42	0.03	0.30	8.36	na	
		SP2	0.40	0.00	0.34	4.81	na	
		RR ($g/m^3/d$)	*3.33*	*0.86*	*1.00*	*-5.50*		
	March 2018 (12 mo)	inlet	5.27	0.08	na	na	1.87	1.48
		outlet	2.74	0.26	na	na	2.29	1.99
		SP1	4.11	0.10	na	na	2.50	1.61
		SP2	0.27	0.06	na	na	2.58	1.76
		SP3	0.15	0.04	na	na	13.06	0.86
		RR ($g/m^3/d$)	*2.34*	*-0.17*			*-0.38*	
Bioreactor 2	October 2017 (3 mo)	inlet	12.70	0.87	1.72	4.35	na	
		outlet	7.24	0.96	1.38	16.10	na	
		SP2	0.33	0.01	0.36	6.91	na	
		RR ($g/m^3/d$)	*8.20*	*-0.13*	*0.50*	*-17.63*		
	March 2018 (8 mo)	inlet	10.93	0.24	na	na	5.27	2.77
		outlet	8.05	0.28	na	na	5.00	3.08
		SP1	2.04	0.11	na	na	6.51	2.30
		SP2	1.61	0.00	na	na	23.74	0.94
		SP3	10.03	0.27	na	na	5.52	2.61
		RR ($g/m^3/d$)	*4.32*	*-0.07*			*0.41*	
Bioreactor 3	October 2017 (9 mo)	inlet	8.20	0.79	2.56	7.48	na	
		outlet	3.53	0.27	2.23	4.08	na	
		SP2	1.42	0.02	1.50	4.34	na	
		RR ($g/m^3/d$)	*7.48*	*0.82*	*0.53*	*5.44*		
	March 2018 (14 mo)	inlet	8.74	1.31	na	na	5.25	1.83
		outlet	3.98	0.76	na	na	5.16	1.79
		SP1	1.42	0.44	na	na	9.67	1.54
		SP2	1.19	0.20	na	na	18.90	0.94
		SP3	3.76	1.08	na	na	5.40	1.98
		RR ($g/m^3/d$)	*7.62*	*0.88*			*0.14*	

Table 3. Gene copy numbers (copies/mL water for water samples, copies/g of dw for biofilm samples), the relationship between DNRA and denitrification potential (*nrf*A/*nir*), the genetic potential for N_2O production (*nir*/*nos*), and the diversity and species richness of *nir*S and *nir*K communities in inlet and outlet water, and in water and biofilm within the bioreactors (sampling points 1-3; SP1-3) in the three bioreactors over the two sampling dates.

Bioreactor	Sampling date	Sampling point	*nir*S	*nir*K	*nosZ*$_I$	*nosZ*$_{II}$	*nrf*A	*nir/nos*	*nrfA/nir*	*nir*S diversity	*nir*S richness	*nir*K diversity	*nir*K richness
Bioreactor 1	October 2017	inlet	6.10E+02	7.28E+03	1.03E+02	1.39E+03	3.30E+02	5.3	0.042	5.2	552.2	3.9	367.1
		SP2_water	6.52E+03	2.42E+05	4.85E+03	4.41E+04	9.43E+03	5.1	0.038	4.2	328.1	4.3	511.6
		SP2_biofilm	7.74E+05	1.96E+06	5.02E+04	6.08E+05	6.74E+04	4.2	0.025	3.9	339.8	4.8	603.3
		outlet	5.21E+03	8.14E+03	1.03E+01	7.55E+03	1.67E+03	1.8	0.125	4.4	256.7	3.7	439.0
	March 2018	inlet	2.26E+05	6.61E+03	5.68E+03	3.86E+02	2.46E+02	38.4	0.001				
		SP1_water	2.42E+07	4.05E+05	1.64E+05	2.99E+04	1.52E+04	127.1	0.001				
		SP2_water	2.07E+07	9.17E+05	4.48E+05	5.05E+04	2.89E+04	43.5	0.001				
		SP3_water	3.31E+07	1.18E+06	5.29E+05	6.21E+04	8.80E+04	58.0	0.003				
		outlet	8.16E+05	1.15E+03	6.49E+03	4.74E+02	5.50E+02	117.4	0.001				
Bioreactor 2	October 2017	inlet	3.71E+02	4.66E+03	3.22E+01	6.71E+02	1.38E+02	7.1	0.027	5.3	614.2	3.7	356.2
		SP2_water	5.85E+05	8.24E+05	8.62E+03	3.43E+05	7.00E+04	4.0	0.050	4.2	423.6	4.4	569.2
		SP2_biofilm	6.92E+05	1.11E+06	6.98E+04	6.56E+05	3.31E+04	2.5	0.018	4.1	436.8	4.4	610.1
		outlet	7.85E+03	8.99E+03	2.02E+01	6.86E+03	8.26E+02	2.4	0.049	4.5	625.3	4.2	293.4
	March 2018	inlet	3.73E+04	4.20E+02	1.75E+03	5.59E+01	3.73E+01	20.9	0.001				
		SP1_water	9.32E+07	3.05E+06	1.11E+06	1.09E+05	1.50E+05	79.1	0.002				

		SP2_water	1.59E+07	2.07E+05	2.22E+05	1.94E+04	2.51E+04	66.6	0.002				
		SP3_water	3.77E+07	1.15E+06	4.46E+05	5.06E+04	4.58E+04	78.2	0.001				
		outlet	9.09E+04	3.14E+02	1.52E+03	1.78E+02	1.87E+03	53.6	0.021				
Bioreactor 3	October 2017	inlet	2.77E+04	6.07E+04	9.53E+02	1.20E+04	2.85E+03	6.8	0.032	3.2	329.0	3.2	173.6
		SP2_water	1.86E+05	7.70E+05	1.27E+04	3.03E+05	6.39E+04	3.0	0.067	4.2	474.8	2.5	168.2
		SP2_biofilm	2.93E+05	1.02E+06	1.81E+04	2.40E+05	5.34E+04	5.1	0.041	4.7	523.3	4.2	567.1
		outlet	6.49E+04	1.12E+05	2.07E+03	5.54E+04	3.34E+03	3.1	0.019	4.5	504.2	2.1	171.0
	March 2018	inlet	6.82E+05	2.91E+04	4.90E+04	3.97E+02	8.60E+02	14.4	0.001				
		SP1_water	5.01E+07	1.83E+06	7.18E+05	6.89E+04	6.02E+04	66.1	0.001				
		SP2_water	2.13E+07	4.00E+05	2.54E+05	2.17E+04	2.03E+04	78.7	0.001				
		SP3_water	3.61E+07	5.19E+05	2.92E+05	3.92E+04	3.02E+04	110.6	0.001				
		outlet	2.19E+06	1.98E+04	4.73E+04	6.34E+02	1.80E+03	46.2	0.001				

Graphical abstract

Highlights

- Dinitrogen producing denitrification the primary pathway in woodchip bioreactors
- Nitrous oxide production can occur when carbon:nitrate is low
- Even 23% of nitrate can be reduced into ammonium under excess carbon
- Bioreactors host active and abundant denitrifier communities of core taxa

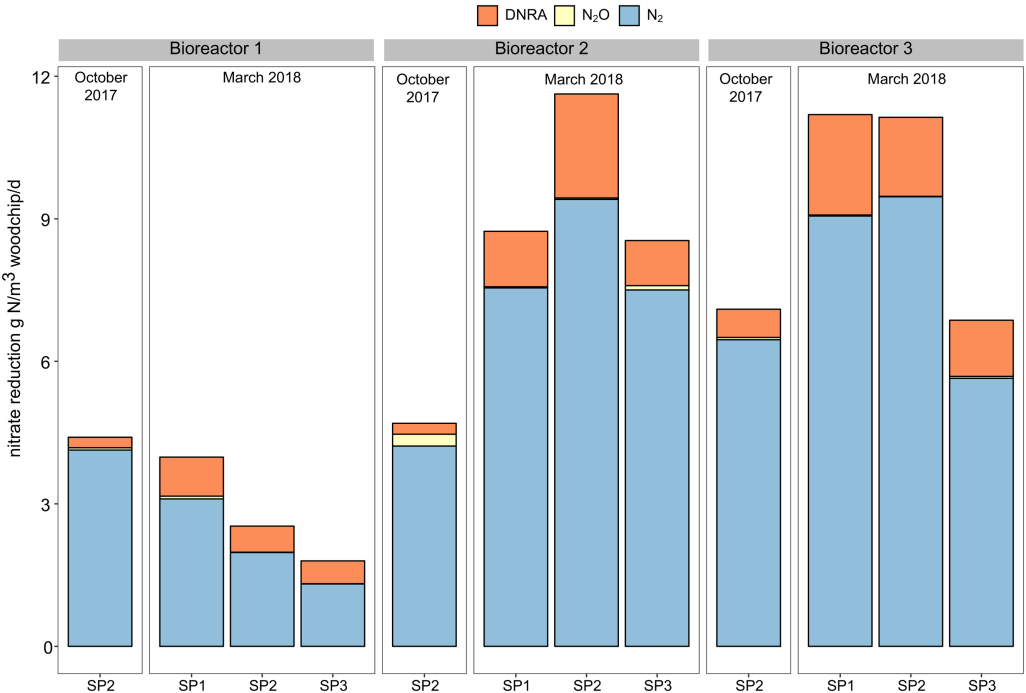
DNRA
N_2O
N_2
Bioreactor 1
Bioreactor 2
Bioreactor 3
October 2017
March 2018
nitrate reduction g N/m3 woodchip/d
12
9
6
3
0
SP1
SP2
SP3

Figure 1

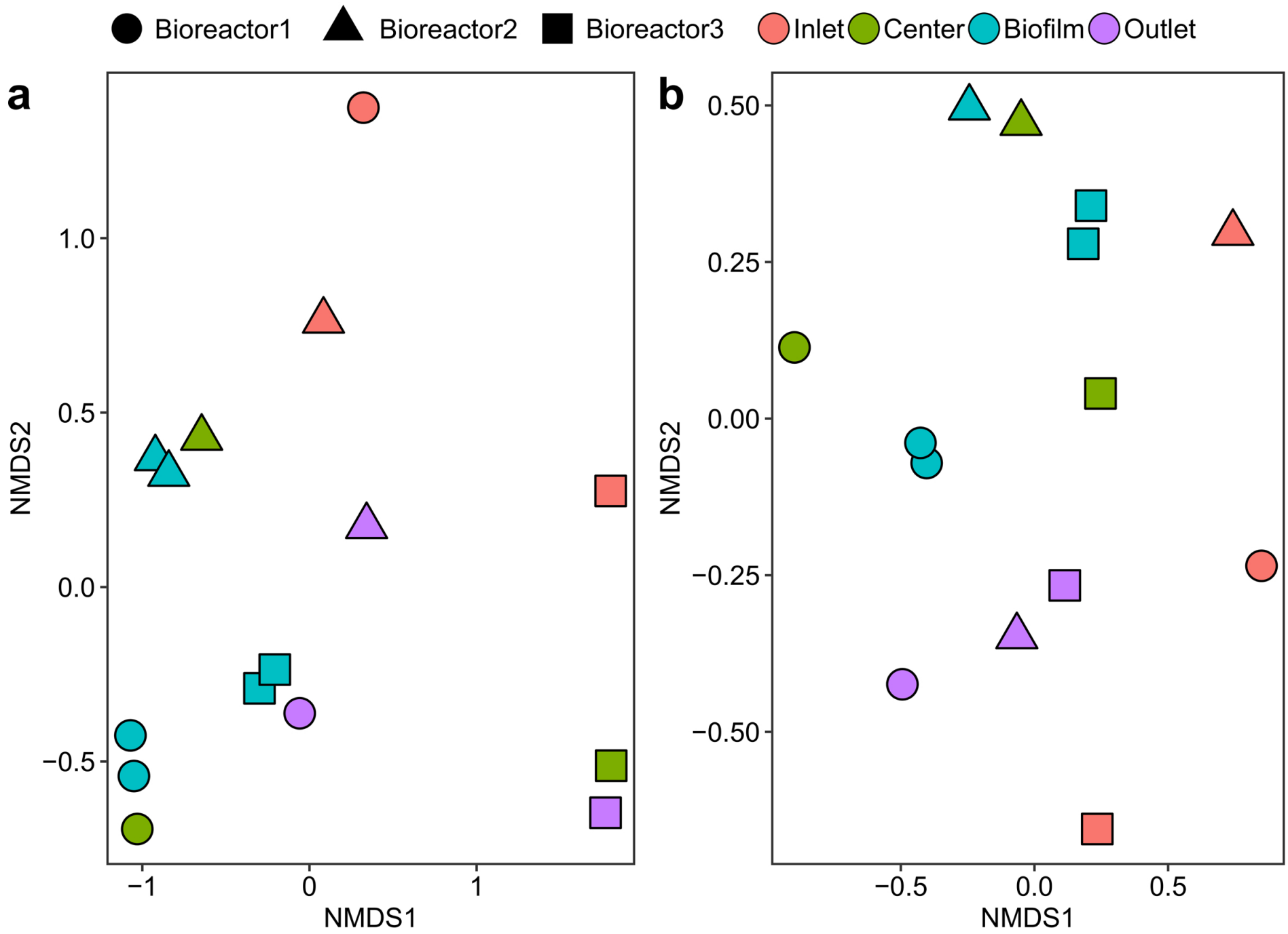
Bioreactor1
Bioreactor2
Bioreactor3
Inlet
Center
Biofilm
Outlet
a
b
NMDS1
NMDS2
1.0
0.5
0.0
−0.5
−1
0
1
0.50
0.25
0.00
−0.25
−0.50
−0.5
0.0
0.5

Figure 2

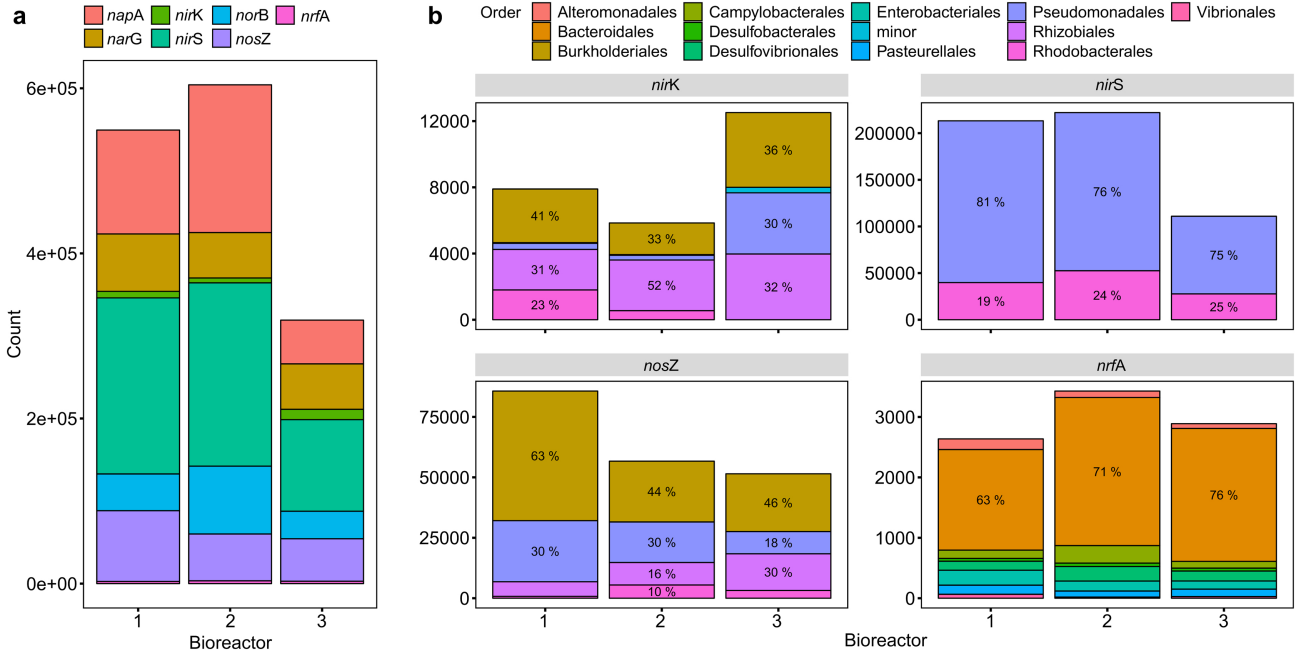
a
napA
narG
nirK
nirS
norB
nosZ
nrfA
Count
6e+05
4e+05
2e+05
0e+00
1
2
3
Bioreactor
b
Order
Alteromonadales
Bacteroidales
Burkholderiales
Campylobacterales
Desulfobacterales
Desulfovibrionales
Enterobacteriales
minor
Pasteurellales
Pseudomonadales
Rhizobiales
Rhodobacterales
Vibrionales
nirK
12000
8000
4000
0
41 %
33 %
36 %
31 %
52 %
30 %
23 %
32 %
nirS
200000
150000
100000
50000
0
81 %
76 %
75 %
19 %
24 %
25 %
nosZ
75000
50000
25000
0
63 %
44 %
46 %
30 %
30 %
18 %
16 %
30 %
10 %
nrfA
3000
2000
1000
0
63 %
71 %
76 %
1
2
3
Bioreactor

Figure 3